New and more dual-mode solitary wave solutions for the Kraenkel-Manna-Merle system incorporating fractal effects

May 22, 2021

Nauman Raza[1], Zara Hassan[1], Asma Rashid Butt[2], Riaz ur Rahman[1], Abdel-Haleem Abdel-Aty[3,4,*]

[1]*Department of Mathematics, University of the Punjab, Quaid-e-Azam Campus, Lahore, Pakistan.*

[2]*Department of Mathematics, University of Engineering and Technology, Lahore, Pakistan.*

[3]*Department of Physics, College of Sciences, University of Bisha, PO Box 344, Bisha 61922, Saudi Arabia.*

[4]*Physics Department, Faculty of Science, Al-Azhar University, Assiut 71524, Egypt.*

Abstract

This paper introduces the fractal Kraenkel-Manna-Merle (KMM) system, that explains nonlinear short wave propagation with zero conductivity for saturated ferromagnetic materials in an external field. The semi inverse technique and the new auxiliary equation method (NAEM) are used to generate a new set of solutions. The proposed methods are more straightforward, succinct, accurate, and simple to calculate dual mode solitary wave solutions. A collection of exact soliton solutions specifically bright, dark, singular-shaped and singular-periodic are generated. The estimated solutions are obtained using constraint conditions and are displayed through 2D, 3D and contour plots with appropriate parametric values. The arbitrary functions in the solutions are chosen as unique functions to generate some novel soliton structures.

OCIS Codes: 060.2310; 060.4510; 060.5530; 190.3270; 190.4370

Keywords: Solitons; Kraenkel-Manna-Merle system; Semi inverse method; New auxiliary equation method.

1 Introduction

In recent years, the study of ferromagnetic materials has wide-ranging applications in several technologies such as information, computers and network communication. Due to this, scientists have given remarkable attention to this research to overcome the requirements of high field intensity storage and massive data with great capacity and speed. For this purpose different attempts have been made to convert the ferromagnetic materials to the nano-scale materials to the size 20-30 nm, with the help of this data in low volume, high density and huge capacity has been processed and transmitted [1–3]. It is important to understand the microstructure and nano-scale characteristics of ferromagnetic media in detail. When it comes to tiny nano-particles, the term magnetization can be considered through a magnetic moment and investigated as homogeneous by these particles. The magnetic moments of ferromagnetic materials can coordinate through dipolar motions [4–6].

Moreover, a particular type of solitary wave solutions to some complicated nonlinear evolution equations that play a vital role in various types of materials are termed as solitons. Such solitary waves have distinct important uses in the fields of fluid dynamics, engineering, elastic media, quantum mechanics, biological sciences, optical fibers, plasma physics, material sciences and many other areas of physics due to its amazing characteristic of stability. Specifically, most of the solitary waves dispersed inelastically and because of radiation phenomena, energy of the wave has lost, as a consequence of which these solitary waves vanished, maintaining their speed and shape after this nonlinear collision. The physical behavior and importance of complex nonlinear evolution processes can be described and interpreted using soliton theory. In order to explore the dynamics of nonlinear complicated process, various effective and efficient techniques for computing solitons and exact solutions have been developed in the literature[7–17].

The spotlight of this piece of research is to present a detailed and readily readable highlighter to a fractal KMM system [18] which is a growing interest for researchers employing semi-inverse algorithm and NAEM [19–23]. In fact, our techniques allow one to acquire fresh exact wave solutions of many nonlinear evolution equations. These can be utilized to produce general exact results that include not only the outcomes obtained as special cases using the procedure but also a collection of new and more popular specific solutions. Some exact solutions with parameters including existing solutions, have been successfully acquired. This article provides the Ritz-like approach combined with the variational method known as He's variational method [24] to find the soliton solution of the KMM system which may help physicists to understand the physical significance of this fractal model. The dynamics of dark and bright solitons can be addressed using techniques[25, 26]. Traveling wave solutions which are developed from existing techniques, may also be practiced by determining the involved parameters in the methods of special values . Many nonlinear mathematical physical models can be constructed using fractal calculus.

The rest of the paper is classified as follows: In section 2, Governing model is given . In section 3, consists of the soliton extraction of the solution with geometrical interpretation by using semi-inverse method. Section 4 composed of soliton solution by NAEM with graphical illustrations. Discussion of the results is in the section 5. In section 6, conclusion of the article is given.

2 Governing system

Kraenkal et al [27] investigated the Maxewell and Landau-Lifshitz-Gilbert equations, short wave propagation in saturated ferromagnetic materials and discovered the following nonlinear evolution system:

$$\begin{aligned} \frac{\partial^2}{\partial T^2}(G+S) &= -\nabla.(\nabla.G) + \nabla^2 G, \\ \frac{\partial S}{\partial T} &= -S \wedge G_{eff} + \frac{\alpha}{a} S \wedge \frac{\partial S}{\partial T}, \end{aligned} \tag{1}$$

where H and G represents magnetization density vector and magnetic induction respectively having no dimensions, whereas α and a are constants and exemplify dimensionless saturation magnetization and Gilbert damping-parameter coorespondingly, where ∇ is divergence for vector field.
Nguepjouo et al.[28] studied a combination of expansion series magnetization density and coordinate transformation in recent years, and transformed the model into the following form:

$$\begin{aligned} y_{xt} - yz_x + by_x &= 0, \\ z_{xt} + yy_x &= 0, \end{aligned} \tag{2}$$

where $z = z(x,t)$ and $y = y(x,t)$ denote the external magnetic field analogous to ferrite and magnetization while x and t are the spatial and temporal components whereas the damping effect is demonstrated by the parameter

b. So, Eq.(2) is referred as Kraenkel-Manna-Merle (KMM) system.
Substituting $b = 0$ different type of soliton solutions like one , two and multiple soliton solutions have been derived by various approaches.

3 Mathematical analysis

By implementing the He's variational principle for innovative solitary wave solutions of Eq.(1) to KMM model. We consider the traveling wave transformation as:

$$\begin{aligned} &y(x,t) = \psi(\eta), \\ &z(x,t) = \phi(\eta), \quad where \qquad \eta = (x - et). \end{aligned} \tag{3}$$

Substituting the transformation in Eq.(2) yields,

$$2e^2\psi'' + 2e_o\psi + \psi^3 = 0, \tag{4}$$

$$\phi^{'} = \frac{\psi^2}{2e} + \frac{e_o}{e}, \tag{5}$$

integration of above equation gives,

$$\phi = \frac{\psi^3}{6e} + \frac{e_o}{e}\psi. \tag{6}$$

In view of [29, 30], a fractal form of KMM model can be written as:

$$2e^2\frac{d}{d\eta^\gamma}\left(\frac{d\psi}{d\eta^\gamma}\right) + 2e_o\psi + \psi^3 = 0, \tag{7}$$

where γ is the fractal dimension value and $\frac{d\psi}{d\eta^\gamma}$ is the fractal derivative, described as:

$$\frac{d\psi}{d\eta^\gamma} = \Gamma(1+\gamma)\lim_{\eta-\eta_o\to\triangle\eta}\frac{\psi(\eta)-\psi(\eta_o)}{(\eta-\eta_o)^\gamma}, \qquad \triangle\,\eta \neq 0. \tag{8}$$

By variational principle [31] the following trial-functional can be constructed as:

$$J = \int L d\eta = \int (K - E) d\eta. \tag{9}$$

The variational formulation of Eq.(7) is given as:

$$J = \int_0^\infty \left[\frac{1}{2}(2e^2)\left(\frac{d\psi}{d\eta^\gamma}\right)^2 - e_o\psi^2 - \frac{\psi^4}{4}\right] d\eta^\gamma, \tag{10}$$

where $K = \frac{1}{2}(2e^2)\left(\frac{d\psi}{d\eta^\gamma}\right)^2$ is the kinetic energy and $E = e_o\psi^2 + \frac{\psi^4}{4}$ is the potential energy.
And

$$L = \frac{1}{2}(2e^2)\left(\frac{d\psi}{d\eta^\gamma}\right)^2 - e_o\psi^2 - \frac{\psi^4}{4}, \tag{11}$$

$$H = \frac{1}{2}(2e^2)\left(\frac{d\psi}{d\eta^\gamma}\right)^2 + e_o\psi^2 + \frac{\psi^4}{4}, \tag{12}$$

are the Lagrangian and Hamiltonian. Using the two scale transformation,

$$Q = \eta^{\gamma}. \tag{13}$$

Eq.(10) can be written as:

$$J = \int_0^{\infty} \left[\frac{1}{2}(2e^2) \left(\frac{d\psi}{dQ} \right)^2 - e_o\psi^2 - \frac{\psi^4}{4} \right] dQ. \tag{14}$$

3.1 Soliton extraction by proposed method

Using Ritz method, one can assume the solitary wave solution as:

$$\psi = D\ sech(MQ), \tag{15}$$

where D and M are constants to be further calculated. putting Eq.(15) into Eq.(14) we have,

$$J = \frac{e^2D^2M}{3} - \frac{e_oD^2}{M} - \frac{D^4}{6M}. \tag{16}$$

Making J stationary with respect to D and M yields,

$$\frac{\partial J}{\partial D} = \frac{2e^2DM}{3} - \frac{2e_oD}{M} - \frac{2D^3}{3M} = 0, \tag{17}$$

$$\frac{\partial J}{\partial M} = \frac{e^2D^2}{3} + \frac{e_oD^2}{M^2} + \frac{D^4}{6M^2} = 0, \tag{18}$$

from Eq.(17) and Eq.(18) we have,

$$D = \pm 2\sqrt{-e_o}, \tag{19}$$

$$M = \pm \frac{\sqrt{-e_o}}{e}. \tag{20}$$

Eq.(15) becomes,

$$\psi = \pm 2\sqrt{-e_o}\ sech\left(\frac{\sqrt{-e_o}}{e}\ Q \right). \tag{21}$$

Substituting the value of ψ in Eq.(6) we have,

$$\phi = \pm \frac{\left[2\sqrt{-e_o}\ sech\left(\frac{\sqrt{-e_o}}{e}\ Q \right) \right]^3}{6e} \pm \frac{e_o}{e} \left[\sqrt{-e_o}\ sech\left(\frac{\sqrt{-e_o}}{e}\ Q \right) \right]. \tag{22}$$

The solution of solitary wave for Eq.(4) is,

$$y(x,t) = \pm 2\sqrt{-e_o}\ sech\left(\frac{\sqrt{-e_o}}{e}\ \eta^{\gamma} \right), \quad where \quad \eta = x - et. \tag{23}$$

$$z(x,t) = \pm \frac{\left[2\sqrt{-e_o}\ sech\left(\frac{\sqrt{-e_o}}{e}\eta^{\gamma} \right) \right]^3}{6e} \pm \frac{e_o}{e} \left[\sqrt{-e_o}\ sech\left(\frac{\sqrt{-e_o}}{e}\eta^{\gamma} \right) \right]. \tag{24}$$

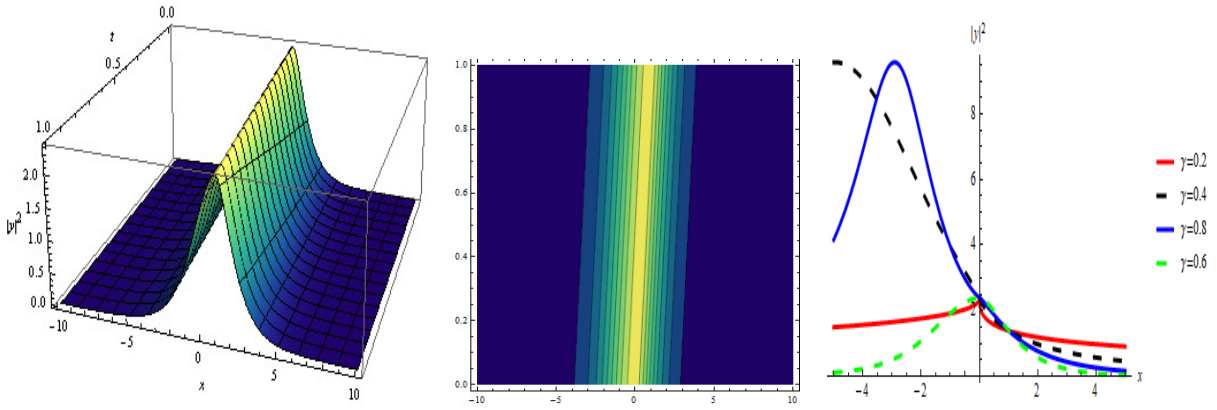

(a) (b) (c)

Figure 1: In these figure, we take $e = 1$, $e_o = -0.6$ and $\gamma = 0.2, 0.4, 0.6, 0.8$. for the solution $|y|^2$. (a) displays the 3D-plot of $|y|^2$ with $\gamma = 0.8$. (b) displays the contour plot of the solution $|y|^2$. (c) displays the 2D-plot of $|y|^2$ with different values of γ.

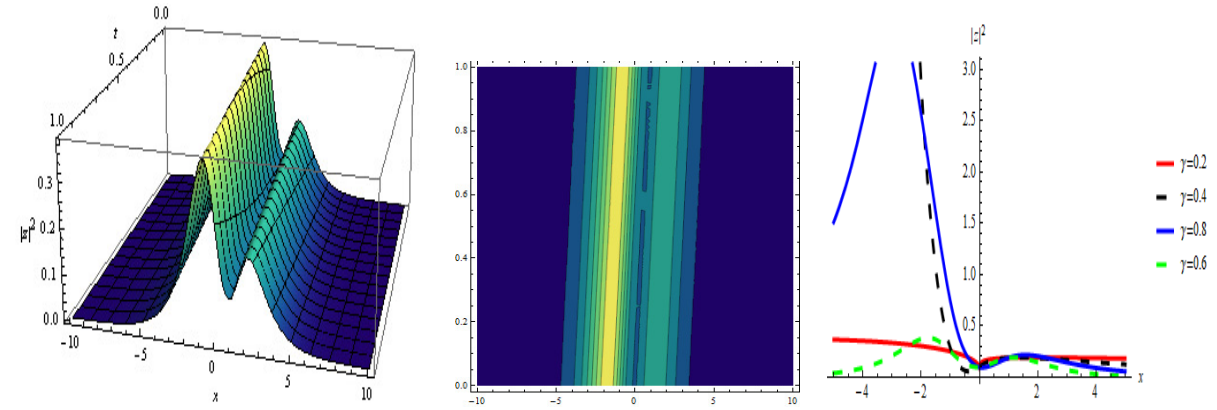

(a) (b) (c)

Figure 2: In these figure, we take $e = 1$, $e_o = -0.6$ and $\gamma = 0.2, 0.4, 0.6, 0.8$. for the solution $|z|^2$. (a) displays the 3D-plot of $|z|^2$ with $\gamma = 0.8$. (b) displays the contour plot of the solution $|z|^2$. (c) displays the 2D-plot of $|z|^2$ with different values of γ.

Also we search another soliton solution in the form,

$$\psi = N\ sech^4(OQ), \tag{25}$$

where N and O are constants to be further calculated. Substituting Eq.(25) in Eq.(14), we have,

$$J = \frac{256e^2N^2O}{315} - \frac{16e_oN^2}{35O} - \frac{512N^4}{6435O}. \tag{26}$$

Making J stationary with respect to N and O yields.

$$\frac{\partial J}{\partial N} = \frac{512e^2NO}{315} - \frac{32e_oN}{35O} - \frac{2048N^3}{6435O} = 0, \tag{27}$$

$$\frac{\partial J}{\partial O} = \frac{256e^2N^2}{315} + \frac{16e_oN^2}{35O^2} + \frac{512N^4}{6435O^2} = 0, \tag{28}$$

from Eq.(27) and Eq.(28) we have,

$$N = \pm\frac{1}{4}\sqrt{-\frac{429}{7}e_o}, \tag{29}$$

$$O = \pm\frac{\sqrt{-3e_o}}{4e}. \tag{30}$$

Eq.(25) becomes,

$$\psi = \pm\frac{1}{4}\sqrt{-\frac{429}{7}e_o}\ sech^4\left(\frac{\sqrt{-3e_o}}{4e}Q\right). \tag{31}$$

Substituting the value of ψ in Eq.(6) we have,

$$\phi = \pm\frac{\left[\frac{1}{4}\sqrt{-\frac{429}{7}e_o}\ sech^4\left(\frac{\sqrt{-3e_o}}{4e}Q\right)\right]^3}{6e} \pm \frac{e_o}{e}\left[\frac{1}{4}\sqrt{-\frac{429}{7}e_o}\ sech^4\left(\frac{\sqrt{-3e_o}}{4e}Q\right)\right]. \tag{32}$$

The solution of solitary wave for Eq.(4) is,

$$y(x,t) = \pm\frac{1}{4}\sqrt{-\frac{429}{7}e_o}\ sech^4\left(\frac{\sqrt{-3e_o}}{4e}\eta^\gamma\right), \quad where \quad \eta = x - et. \tag{33}$$

$$z(x,t) = \pm\frac{\left[\frac{1}{4}\sqrt{-\frac{429}{7}e_o}\ sech^4\left(\frac{\sqrt{-3e_o}}{4e}\eta^\gamma\right)\right]^3}{6e} \pm \frac{e_o}{e}\left[\frac{1}{4}\sqrt{-\frac{429}{7}e_o}\ sech^4\left(\frac{\sqrt{-3e_o}}{4e}\eta^\gamma\right)\right]. \tag{34}$$

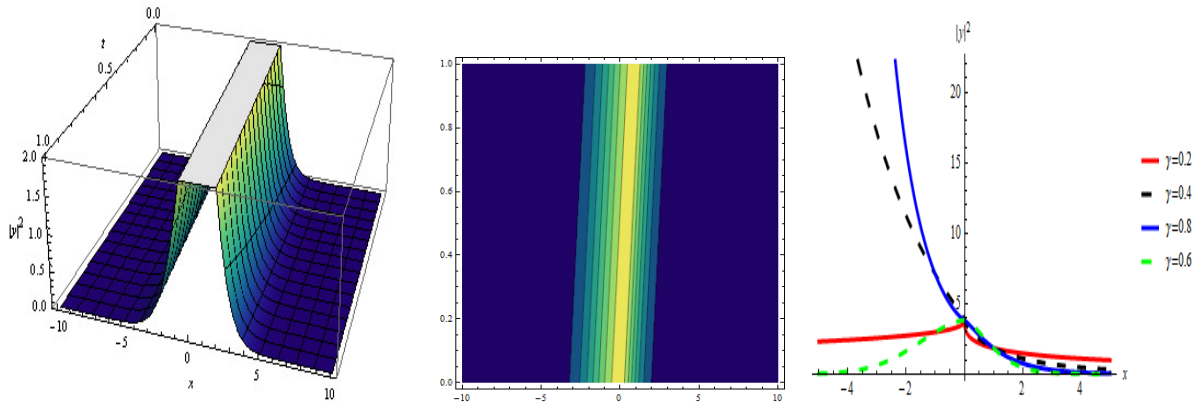

(a) (b) (c)

Figure 3: In these figure, we take $e = 1$, $e_o = -1$ and $\gamma = 0.2, 0.4, 0.6, 0.8$. for the solution $|y|^2$. (a) displays the 3D-plot of $|y|^2$ with $\gamma = 0.8$. (b) displays the contour plot of the solution $|y|^2$. (c) displays the 2D-plot of $|y|^2$ with different values of γ.

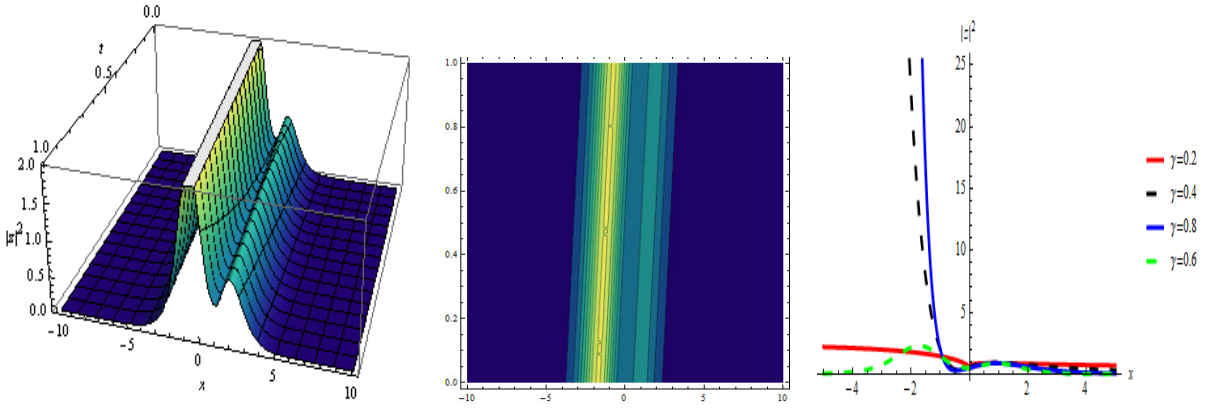

(a) (b) (c)

Figure 4: In these figure, we take $e = 1$, $e_o = -1$ and $\gamma = 0.2, 0.4, 0.6, 0.8$. for the solution $|z|^2$. (a) displays the 3D-plot of $|z|^2$ with $\gamma = 0.8$. (b) displays the contour plot of the solution $|z|^2$. (c) displays the 2D-plot of $|z|^2$ with different values of γ.

4 Key points of the NAEM

Consider the general structure of NLPDE in the following expression:

$$Q(u, u_x, uu_x, u_t, u_{xx}, uu_{xx}, u_{tt}, ...) = 0, \tag{35}$$

where Q is a polynomial function of u and their derivatives with respect to two independent variables x and t. Use the transformation of single variable $\eta = x - c_0 t$ to reduce the Eq.(35) into a simpler ordinary differential equation of the following form:

$$R(\psi, \psi^{'}, \psi^{''}, \psi\psi^{''}, ...) = 0. \tag{36}$$

Here, R is a polynomial function involving the linear and nonlinear terms and the superscripts of ψ show ordinary derivative of ψ with respect to η. Using the concept of NAEM, the initial solution of Eq.(36) can be assumed in the following way:

$$\psi(\eta) = \sum_{i=0}^{M} c_i \beta^{if(\eta)}, \tag{37}$$

with satisfying the auxiliary equation

$$f^{'}(\eta) = \frac{1}{ln(\beta)}\left(\mu\beta^{-f(\eta)} + \lambda + \nu\beta^{f(\eta)}\right). \tag{38}$$

where c_0, c_1, c_2, ..., c_M are coefficients to be determined such that $c_M \neq 0$. Now, we find the value of M with the help of balancing principle which states that we can find the value of M by comparing the highest linear and nonlinear terms involved in Eq.(4).

Now, putting Eq.(37) into Eq.(4) and performing few steps of algebra, yields a system of algebraic equations in $\beta^{f(\eta)}$.

The family of solutions of Eq.(38) can be obtained as follows:

Family 1: When $\lambda^2 - 4\mu\nu < 0$ **and** $\nu \neq 0$,

$$\beta^{f(\eta)} = \frac{-\lambda}{2\nu} + \frac{\sqrt{4\mu\nu - \lambda^2}}{2\nu}\ tan\bigg(\frac{\sqrt{4\mu\nu - \lambda^2}}{2}\ \eta\bigg), \tag{39}$$

$$\beta^{f(\eta)} = \frac{-\lambda}{2\nu} - \frac{\sqrt{4\mu\nu - \lambda^2}}{2\nu}\ cot\bigg(\frac{\sqrt{4\mu\nu - \lambda^2}}{2}\ \eta\bigg). \tag{40}$$

Family 2: When $\lambda^2 - 4\mu\nu > 0$ and $\nu \neq 0$,

$$\beta^{f(\eta)} = \frac{-\lambda}{2\nu} - \frac{\sqrt{\lambda^2 - 4\mu\nu}}{2\nu}\ tanh\bigg(\frac{\sqrt{\lambda^2 - 4\mu\nu}}{2}\ \eta\bigg), \tag{41}$$

$$\beta^{f(\eta)} = \frac{-\lambda}{2\nu} - \frac{\sqrt{\lambda^2 - 4\mu\nu}}{2\nu}\ coth\bigg(\frac{\sqrt{\lambda^2 - 4\mu\nu}}{2}\ \eta\bigg). \tag{42}$$

Family 3: When $\lambda^2 + 4\mu^2 < 0$ and $\nu \neq 0$ and $\nu = -\mu$,

$$\beta^{f(\eta)} = \frac{\lambda}{2\mu} - \frac{\sqrt{-4\mu^2 - \lambda^2}}{2\mu}\ tan\bigg(\frac{\sqrt{-4\mu^2 - \lambda^2}}{2}\ \eta\bigg), \tag{43}$$

$$\beta^{f(\eta)} = \frac{\lambda}{2\nu} + \frac{\sqrt{-4\mu^2 - \lambda^2}}{2\mu}\ cot\bigg(\frac{\sqrt{-4\mu^2 - \lambda^2}}{2}\ \eta\bigg). \tag{44}$$

Family 4: When $\lambda^2 + 4\mu^2 < 0$ and $\nu \neq 0$ and $\nu = -\mu$,

$$\beta^{f(\eta)} = \frac{\lambda}{2\mu} + \frac{\sqrt{4\mu^2 + \lambda^2}}{2\mu}\ tanh\bigg(\frac{\sqrt{4\mu^2 + \lambda^2}}{2}\ \eta\bigg), \tag{45}$$

$$\beta^{f(\eta)} = \frac{\lambda}{2\mu} + \frac{\sqrt{4\mu^2 + \lambda^2}}{2\mu}\ coth\bigg(\frac{\sqrt{4\mu^2 + \lambda^2}}{2}\ \eta\bigg). \tag{46}$$

Family 5: When $\lambda^2 - 4\mu^2 < 0$ and $\nu = \mu$,

$$\beta^{f(\eta)} = \frac{-\lambda}{2\mu} + \frac{\sqrt{4\mu^2 - \lambda^2}}{2\mu}\ tan\bigg(\frac{\sqrt{4\mu^2 - \lambda^2}}{2}\ \eta\bigg), \tag{47}$$

$$\beta^{f(\eta)} = \frac{-\lambda}{2\mu} - \frac{\sqrt{4\mu^2 - \lambda^2}}{2\mu}\ cot\bigg(\frac{\sqrt{4\mu^2 - \lambda^2}}{2}\ \eta\bigg). \tag{48}$$

Family 6: When $\lambda^2 - 4\mu^2 > 0$ and $\nu = \mu$,

$$\beta^{f(\eta)} = \frac{-\lambda}{2\mu} - \frac{\sqrt{-4\mu^2 + \lambda^2}}{2\mu}\ tanh\frac{\sqrt{-4\mu^2 + \lambda^2}}{2}\ \eta\bigg), \tag{49}$$

$$\beta^{f(\eta)} = \frac{-\lambda}{2\mu} - \frac{\sqrt{-4\mu^2 + \lambda^2}}{2\mu}\ coth\bigg(\frac{\sqrt{-4\mu^2 + \lambda^2}}{2}\ \eta\bigg). \tag{50}$$

Family 7: When $\lambda^2 = 4\mu\nu$,

$$\beta^{f(\eta)} = -\frac{2 + \lambda\eta}{2\nu\eta}. \tag{51}$$

Family 8: When $\nu\mu < 0$, $\lambda = 0$ and $\nu \neq 0$,

$$\beta^{f(\eta)} = -\sqrt{\frac{-\mu}{\nu}}\ tanh(\sqrt{-\nu\mu}\ \eta), \tag{52}$$

$$\beta^{f(\eta)} = -\sqrt{\frac{-\mu}{\nu}}\ coth(\sqrt{-\nu\mu}\ \eta). \tag{53}$$

Family 9: When $\lambda = 0$ and $\mu = -\nu$,

$$\beta^{f(\eta)} = \frac{1 + e^{-2\nu\eta}}{-1 + e^{-2\nu\eta}}. \tag{54}$$

Family 10: When $\mu = \nu = 0$,

$$\beta^{f(\eta)} = cosh(\lambda\ \eta) + sinh(\lambda\ \eta). \tag{55}$$

Family 11: When $\mu = \lambda = K$ and $\nu = 0$,

$$\beta^{f(\eta)} = e^{K\eta} - 1. \tag{56}$$

Family 12: When $\nu = \lambda = K$ and $\mu = 0$,

$$\beta^{f(\eta)} = \frac{e^{K\eta}}{1 - e^{K\eta}}. \tag{57}$$

Family 13: When $\lambda = \mu + \nu$,

$$\beta^{f(\eta)} = -\frac{1 - \mu e^{(\mu-\nu)\eta}}{1 - \nu e^{(\mu-\nu)\eta}}. \tag{58}$$

Family 14: When $\lambda = -(\mu + \nu)$,

$$\beta^{f(\eta)} = \frac{\mu - e^{(\mu-\nu)\eta}}{\nu - e^{(\mu-\nu)\eta}}. \tag{59}$$

Family 15: When $\mu = 0$,

$$\beta^{f(\eta)} = \frac{\lambda e^{\lambda\ \eta}}{1 - \nu e^{\lambda\eta}}. \tag{60}$$

Family 16: When $\lambda = \mu = \nu \neq 0$,

$$\beta^{f(\eta)} = \frac{1}{2}\left[\sqrt{3}\ tan\ (\frac{\sqrt{3}}{2}\mu\ \eta) - 1\right]. \tag{61}$$

Family 17: When $\lambda = \nu = 0$,

$$\beta^{f(\eta)} = \mu\eta. \tag{62}$$

Family 18: When $\lambda = \mu = 0$,

$$\beta^{f(\eta)} = -\frac{1}{\nu\eta}. \tag{63}$$

Family 19: When $\mu = \nu$ and $\lambda = 0$,

$$\beta^{f(\eta)} = tan(\mu\ \eta). \tag{64}$$

Family 20: When $\nu = 0$,

$$\beta^{f(\eta)} = e^{\lambda\eta} - \frac{m}{n}. \tag{65}$$

4.1 Application of NAEM

The index M is to be calculated by employing the homogeneous system to higher order derivative with nonlinear term in Eq.(4), which results $M = 1$. Hence, the Eq.(37) has the form:

$$\psi(\xi) = c_0 + c_1\beta^{f(\xi)}. \tag{66}$$

Now, substituting Eq.(66) into Eq.(4), a system of equations is attained. On solving the produced system via Maple, it yields:

$$c_0 = \sqrt{2}\ \lambda\ \Pi, \quad c_1 = 2\sqrt{2}\ \Pi\ \nu, \quad e = \sqrt{-\frac{2e_0}{4\mu\nu - \lambda^2}}, \tag{67}$$

where

$$\Pi = \sqrt{\frac{e_0}{4\mu\nu - \lambda^2}}. \tag{68}$$

Now substituting the obtained solution into Eq.(66), we get the following:

$$\psi(\eta) = \sqrt{2}\Pi\Big(\lambda + 2\nu\beta^{f(\eta^\gamma)}\Big). \tag{69}$$

Substituting the value of ψ into Eq.(6) we have,

$$\phi = \frac{\Big[\sqrt{2}\Pi\Big(\lambda + 2\nu\beta^{f(\eta^\gamma)}\Big)\Big]^3}{6e} + \frac{e_o}{e}\Big[\sqrt{2}\Pi\Big(\lambda + 2\nu\beta^{f(\eta^\gamma)}\Big)\Big]. \tag{70}$$

The solution of solitary wave for Eq.(4) is:

$$y(x,t) = \sqrt{2}\Pi\Big(\lambda + 2\nu\beta^{f(\eta^\gamma)}\Big), \quad where \ \ \eta = x - et \tag{71}$$

and

$$z(x,t) = \frac{\Big[\sqrt{2}\Pi\Big(\lambda + 2\nu\beta^{f(\eta^\gamma)}\Big)\Big]^3}{6e} \pm \frac{e_o}{e}\Big[\sqrt{2}\Pi\Big(\lambda + 2\nu\beta^{f(\eta^\gamma)}\Big)\Big]. \tag{72}$$

By substituting the solutions specified by Eq.(38) into Eq.(71) and Eq.(72), the solutions retrieved are:
For Family 1: When $\lambda^2 - 4\mu\nu < 0$ **and** $\nu \neq 0$,

$$y_{1,1}(x,t) = \sqrt{2}\Pi\Bigg[\sqrt{4\mu\nu-\lambda^2}\ tan\Bigg(\frac{\sqrt{4\mu\nu-\lambda^2}}{2}\ \eta^\gamma\Bigg)\Bigg], \tag{73}$$

$$y_{1,2}(x,t) = -\sqrt{2}\Pi\Bigg[\sqrt{4\mu\nu-\lambda^2}\ cot\Bigg(\frac{\sqrt{4\mu\nu-\lambda^2}}{2}\ \eta^\gamma\Bigg)\Bigg], \tag{74}$$

$$z_{1,1}(x,t) = \frac{\Bigg[\sqrt{2}\Pi\Bigg[\sqrt{4\mu\nu-\lambda^2}\ tan\Bigg(\frac{\sqrt{4\mu\nu-\lambda^2}}{2}\ \eta^\gamma\Bigg)\Bigg]\Bigg]^3}{6e} + \frac{e_o}{e}\Bigg[\sqrt{2}\Pi\Bigg[\sqrt{4\mu\nu-\lambda^2}\ tan\Bigg(\frac{\sqrt{4\mu\nu-\lambda^2}}{2}\ \eta^\gamma\Bigg)\Bigg]\Bigg], \tag{75}$$

$$z_{1,2}(x,t) = \frac{\Bigg[-\sqrt{2}\Pi\Bigg[\sqrt{4\mu\nu-\lambda^2}\ cot\Bigg(\frac{\sqrt{4\mu\nu-\lambda^2}}{2}\ \eta^\gamma\Bigg)\Bigg]\Bigg]^3}{6e} + \frac{e_o}{e}\Bigg[-\sqrt{2}\Pi\Bigg[\sqrt{4\mu\nu-\lambda^2}\ cot\Bigg(\frac{\sqrt{4\mu\nu-\lambda^2}}{2}\ \eta^\gamma\Bigg)\Bigg]\Bigg]. \tag{76}$$

For Family 2: When $\lambda^2 - 4\mu\nu > 0$ and $\nu \neq 0$,

$$y_{2,1}(x,t) = -\sqrt{2}\Pi\Bigg[\sqrt{\lambda^2-4\mu\nu}\ tanh\Bigg(\frac{\sqrt{\lambda^2-4\mu\nu}}{2}\ \eta^\gamma\Bigg)\Bigg], \tag{77}$$

$$y_{2,2}(x,t) = -\sqrt{2}\Pi\Bigg[\sqrt{\lambda^2-4\mu\nu}\ coth\Bigg(\frac{\sqrt{\lambda^2-4\mu\nu}}{2}\ \eta^\gamma\Bigg)\Bigg], \tag{78}$$

$$z_{2,1}(x,t) = \frac{\Bigg[-\sqrt{2}\Pi\Bigg[\sqrt{\lambda^2-4\mu\nu}\ tanh\Bigg(\frac{\sqrt{\lambda^2-4\mu\nu}}{2}\ \eta^\gamma\Bigg)\Bigg]\Bigg]^3}{6e} + \frac{e_o}{e}\Bigg[-\sqrt{2}\Pi\Bigg[\sqrt{\lambda^2-4\mu\nu}\ tanh\Bigg(\frac{\sqrt{\lambda^2-4\mu\nu}}{2}\ \eta^\gamma\Bigg)\Bigg]\Bigg], \tag{79}$$

$$z_{2,2}(x,t) = \frac{\Bigg[-\sqrt{2}\Pi\Bigg[\sqrt{\lambda^2-4\mu\nu}\ coth\Bigg(\frac{\sqrt{\lambda^2-4\mu\nu}}{2}\ \eta^\gamma\Bigg)\Bigg]\Bigg]^3}{6e} + \frac{e_o}{e}\Bigg[-\sqrt{2}\Pi\Bigg[\sqrt{\lambda^2-4\mu\nu}\ coth\Bigg(\frac{\sqrt{\lambda^2-4\mu\nu}}{2}\ \eta^\gamma\Bigg)\Bigg]\Bigg]. \tag{80}$$

For Family 3: When $\lambda^2 + 4\mu\nu < 0$, $\nu \neq 0$ and $\nu = -\mu$,

$$y_{3,1}(x,t) = \sqrt{2}\Pi\left[\sqrt{-4\mu^2-\lambda^2}\ tan\left(\frac{\sqrt{-4\mu^2-\lambda^2}}{2}\ \eta^\gamma\right)\right], \tag{81}$$

$$y_{3,2}(x,t) = -\sqrt{2}\Pi\left[\sqrt{-4\mu^2-\lambda^2}\ cot\left(\frac{\sqrt{-4\mu^2-\lambda^2}}{2}\ \eta^\gamma\right)\right], \tag{82}$$

$$z_{3,1}(x,t) = \frac{\left[\sqrt{2}\Pi\left[\sqrt{-4\mu^2-\lambda^2}\ tan\left(\frac{\sqrt{-4\mu^2-\lambda^2}}{2}\ \eta^\gamma\right)\right]\right]^3}{6e} + \frac{e_o}{e}\left[\sqrt{2}\Pi\left[\sqrt{-4\mu^2-\lambda^2}\ tan\left(\frac{\sqrt{-4\mu^2-\lambda^2}}{2}\ \eta^\gamma\right)\right]\right], \tag{83}$$

$$z_{3,2}(x,t) = \frac{\left[-\sqrt{2}\Pi\left[\sqrt{-4\mu^2-\lambda^2}\ cot\left(\frac{\sqrt{-4\mu^2-\lambda^2}}{2}\ \eta^\gamma\right)\right]\right]^3}{6e} + \frac{e_o}{e}\left[-\sqrt{2}\Pi\left[\sqrt{-4\mu^2-\lambda^2}\ cot\left(\frac{\sqrt{-4\mu^2-\lambda^2}}{2}\ \eta^\gamma\right)\right]\right]. \tag{84}$$

For Family 4: When $\lambda^2 + 4\mu\nu > 0$, $\nu \neq 0$ and $\nu = -\mu$,

$$y_{4,1}(x,t) = -\sqrt{2}\Pi\left[\sqrt{4\mu^2+\lambda^2}\ tanh\left(\frac{\sqrt{4\mu^2+\lambda^2}}{2}\ \eta^\gamma\right)\right], \tag{85}$$

$$y_{4,2}(x,t) = -\sqrt{2}\Pi\left[\sqrt{4\mu^2+\lambda^2}\ coth\left(\frac{\sqrt{4\mu^2+\lambda^2}}{2}\ \eta^\gamma\right)\right], \tag{86}$$

$$z_{4,1}(x,t) = \frac{\left[-\sqrt{2}\Pi\left[\sqrt{4\mu^2+\lambda^2}\ tanh\left(\frac{\sqrt{4\mu^2+\lambda^2}}{2}\ \eta^\gamma\right)\right]\right]^3}{6e} + \frac{e_o}{e}\left[-\sqrt{2}\Pi\left[\sqrt{4\mu^2+\lambda^2}\ tanh\left(\frac{\sqrt{4\mu^2+\lambda^2}}{2}\ \eta^\gamma\right)\right]\right], \tag{87}$$

$$z_{4,2}(x,t) = \frac{\left[-\sqrt{2}\Pi\left[\sqrt{4\mu^2+\lambda^2}\ coth\left(\frac{\sqrt{4\mu^2+\lambda^2}}{2}\ \eta^\gamma\right)\right]\right]^3}{6e} + \frac{e_o}{e}\left[-\sqrt{2}\Pi\left[\sqrt{4\mu^2+\lambda^2}\ coth\left(\frac{\sqrt{4\mu^2+\lambda^2}}{2}\ \eta^\gamma\right)\right]\right]. \tag{88}$$

For Family 5: When $\lambda^2 - 4\mu^2 < 0$ and $\nu = \mu$,

$$y_{5,1}(x,t) = \sqrt{2}\Pi\left[\sqrt{4\mu^2-\lambda^2}\ tan\left(\frac{\sqrt{4\mu^2-\lambda^2}}{2}\ \eta^\gamma\right)\right], \tag{89}$$

$$y_{5,2}(x,t) = -\sqrt{2}\Pi\left[\sqrt{4\mu^2-\lambda^2}\ cot\left(\frac{\sqrt{4\mu^2-\lambda^2}}{2}\ \eta^\gamma\right)\right], \tag{90}$$

$$z_{5,1}(x,t) = \frac{\left[\sqrt{2}\Pi\left[\sqrt{4\mu^2-\lambda^2}\ tan\left(\frac{\sqrt{4\mu^2-\lambda^2}}{2}\ \eta^\gamma\right)\right]\right]^3}{6e} + \frac{e_o}{e}\left[\sqrt{2}\Pi\left[\sqrt{4\mu^2-\lambda^2}\ tan\left(\frac{\sqrt{4\mu^2-\lambda^2}}{2}\ \eta^\gamma\right)\right]\right], \tag{91}$$

$$z_{5,2}(x,t) = \frac{\left[-\sqrt{2}\Pi\left[\sqrt{4\mu^2-\lambda^2}\ cot\left(\frac{\sqrt{4\mu^2-\lambda^2}}{2}\ \eta^\gamma\right)\right]\right]^3}{6e} + \frac{e_o}{e}\left[-\sqrt{2}\Pi\left[\sqrt{4\mu^2-\lambda^2}\ cot\left(\frac{\sqrt{4\mu^2-\lambda^2}}{2}\ \eta^\gamma\right)\right]\right]. \tag{92}$$

For Family 6: When $\lambda^2 - 4\mu^2 > 0$ and $\nu = \mu$,

$$y_{6,1}(x,t) = -\sqrt{2}\Pi\left[\sqrt{-4\mu^2+\lambda^2}\ tanh\left(\frac{\sqrt{-4\mu^2+\lambda^2}}{2}\ \eta^\gamma\right)\right], \tag{93}$$

$$y_{6,2}(x,t) = -\sqrt{2}\Pi\left[\sqrt{-4\mu^2+\lambda^2}\ coth\left(\frac{\sqrt{-4\mu^2+\lambda^2}}{2}\ \eta^\gamma\right)\right], \tag{94}$$

$$z_{6,1}(x,t) = \frac{\left[\sqrt{2}\Pi\left[-\sqrt{2}\Pi\left[\sqrt{-4\mu^2+\lambda^2}\ tanh\left(\frac{\sqrt{-4\mu^2+\lambda^2}}{2}\ \eta^\gamma\right)\right]\right]\right]^3}{6e} + \frac{e_o}{e}\left[-\sqrt{2}\Pi\left[\sqrt{-4\mu^2+\lambda^2}\ tanh\left(\frac{\sqrt{-4\mu^2+\lambda^2}}{2}\ \eta^\gamma\right)\right]\right], \tag{95}$$

$$z_{6,2}(x,t) = \frac{\left[-\sqrt{2}\Pi\left[\sqrt{-4\mu^2+\lambda^2}\ coth\left(\frac{\sqrt{-4\mu^2+\lambda^2}}{2}\ \eta^\gamma\right)\right]\right]^3}{6e} + \frac{e_o}{e}\left[-\sqrt{2}\Pi\left[\sqrt{-4\mu^2+\lambda^2}\ coth\left(\frac{\sqrt{-4\mu^2+\lambda^2}}{2}\ \eta^\gamma\right)\right]\right]. \tag{96}$$

For Family 7: When $\lambda^2 = 4\mu\nu$,

$$y_7(x,t) = 2\sqrt{2}\Pi\left[\frac{\lambda\eta^\gamma - 1}{\eta^\gamma}\right], \tag{97}$$

$$z_7(x,t) = \frac{\left[2\sqrt{2}\Pi\left[\frac{\lambda\eta^\gamma-1}{\eta^\gamma}\right]\right]^3}{6e} + \frac{e_o}{e}\left[2\sqrt{2}\Pi\left[\frac{\lambda\eta^\gamma - 1}{\eta^\gamma}\right]\right]. \tag{98}$$

For Family 8: When $\mu\nu < 0$, $\lambda = 0$ and $\nu \neq 0$,

$$y_{8,1}(x,t) = -2\sqrt{2}\Pi\left[\sqrt{-\mu\nu}tanh\left(\sqrt{-\nu\mu}\ \eta^{\gamma}\right)\right], \tag{99}$$

$$y_{8,2}(x,t) = -2\sqrt{2}\Pi\left[\sqrt{-\mu\nu}coth\left(\sqrt{-\nu\mu}\ \eta^{\gamma}\right)\right], \tag{100}$$

$$z_{8,1}(x,t) = \frac{\left[\sqrt{2}\Pi\left[-2\sqrt{2}\Pi\left[\sqrt{-\mu\nu}tanh\left(\sqrt{-\nu\mu}\ \eta^{\gamma}\right)\right]\right]\right]^{3}}{6e} + \frac{e_o}{e}\left[-2\sqrt{2}\Pi\left[\sqrt{-\mu\nu}tanh\left(\sqrt{-\nu\mu}\ \eta^{\gamma}\right)\right]\right], \tag{101}$$

$$z_{8,2}(x,t) = \frac{\left[-2\sqrt{2}\Pi\left[\sqrt{-\mu\nu}coth\left(\sqrt{-\nu\mu}\ \eta^{\gamma}\right)\right]\right]^{3}}{6e} + \frac{e_o}{e}\left[-2\sqrt{2}\Pi\left[\sqrt{-\mu\nu}coth\left(\sqrt{-\nu\mu}\ \eta^{\gamma}\right)\right]\right]. \tag{102}$$

For Family 9: When $\lambda = 0$ and $\mu = -\nu$,

$$y_9(x,t) = 2\sqrt{2}\Pi\nu\left[\frac{1+e^{-2\nu\eta^{\gamma}}}{-1+e^{-2\nu\eta^{\gamma}}}\right], \tag{103}$$

$$z_9(x,t) = \frac{\left[2\sqrt{2}\Pi\nu\left[\frac{1+e^{-2\nu\eta^{\gamma}}}{-1+e^{-2\nu\eta^{\gamma}}}\right]\right]^{3}}{6e} + \frac{e_o}{e}\left[2\sqrt{2}\Pi\nu\left[\frac{1+e^{-2\nu\eta^{\gamma}}}{-1+e^{-2\nu\eta^{\gamma}}}\right]\right]. \tag{104}$$

For Family 12: When $\nu = \lambda = K$ and $\mu = 0$,

$$y_{12}(x,t) = \sqrt{2}\Pi\left[K + 2K\left(\frac{e^{K\eta^{\gamma}}}{1-e^{K\eta^{\gamma}}}\right)\right], \tag{105}$$

$$z_{12}(x,t) = \frac{\left[\sqrt{2}\Pi\left[K + 2K\left(\frac{e^{K\eta^{\gamma}}}{1-e^{K\eta^{\gamma}}}\right)\right]\right]^{3}}{6e} + \frac{e_o}{e}\left[\sqrt{2}\Pi\left[K + 2K\left(\frac{e^{K\eta^{\gamma}}}{1-e^{K\eta^{\gamma}}}\right)\right]\right]. \tag{106}$$

For Family 13: When $\lambda = \mu + \nu$,

$$v_{13}(x,t) = \sqrt{2}\Pi\left[\mu + \nu - 2\nu\left(\frac{1-\mu e^{(\mu-\nu)\eta^{\gamma}}}{1-\nu e^{(\mu-\nu)\eta^{\gamma}}}\right)\right], \tag{107}$$

$$z_{13}(x,t) = \frac{\left[\sqrt{2}\Pi\left[\mu + \nu - 2\nu\left(\frac{1-\mu e^{(\mu-\nu)\eta^{\gamma}}}{1-\nu e^{(\mu-\nu)\eta^{\gamma}}}\right)\right]\right]^{3}}{6e} + \frac{e_o}{e}\left[\sqrt{2}\Pi\left[\mu + \nu - 2\nu\left(\frac{1-\mu e^{(\mu-\nu)\eta^{\gamma}}}{1-\nu e^{(\mu-\nu)\eta^{\gamma}}}\right)\right]\right]. \tag{108}$$

For Family 14: When $\lambda = -(\mu + \nu)$,

$$y_{14}(x,t) = \sqrt{2}\Pi\Big[-\mu - \nu + 2\nu\Big(\frac{\mu - e^{(\mu-\nu)\eta^\gamma}}{\nu - e^{(\mu-\nu)\eta^\gamma}}\Big)\Big], \tag{109}$$

$$z_{14}(x,t) = \frac{\Big[\sqrt{2}\Pi\Big[-\mu - \nu + 2\nu\Big(\frac{\mu - e^{(\mu-\nu)\eta^\gamma}}{\nu - e^{(\mu-\nu)\eta^\gamma}}\Big)\Big]\Big]^3}{6e} + \frac{e_o}{e}\Big[\sqrt{2}\Pi\Big[-\mu - \nu + 2\nu\Big(\frac{\mu - e^{(\mu-\nu)\eta^\gamma}}{\nu - e^{(\mu-\nu)\eta^\gamma}}\Big)\Big]\Big]. \tag{110}$$

For Family 15: When $\mu = 0$,

$$y_{15}(x,t) = \sqrt{2}\Pi\Big[\lambda + 2\nu\Big(\frac{\lambda e^{\lambda\eta^\gamma}}{1 - \nu e^{\lambda\eta^\gamma}}\Big)\Big], \tag{111}$$

$$z_{15}(x,t) = \frac{\Big[\sqrt{2}\Pi\Big[\lambda + 2\nu\Big(\frac{\lambda e^{\lambda\eta^\gamma}}{1-\nu e^{\lambda\eta^\gamma}}\Big)\Big]\Big]^3}{6e} + \frac{e_o}{e}\Big[\sqrt{2}\Pi\Big[\lambda + 2\nu\Big(\frac{\lambda e^{\lambda\eta^\gamma}}{1 - \nu e^{\lambda\eta^\gamma}}\Big)\Big]\Big]. \tag{112}$$

For Family 16: When $\lambda = \mu = \nu \neq 0$,

$$y_{16}(x,t) = \Pi\Big[\lambda + \nu\Big\{\sqrt{3}tan\Big(\frac{\sqrt{3}}{2}\ \mu\ \eta^\gamma\Big) - 1\Big\}\Big], \tag{113}$$

$$z_{16}(x,t) = \frac{\Big[\Pi\Big[\lambda + \nu\Big\{\sqrt{3}tan\Big(\frac{\sqrt{3}}{2}\ \mu\ \eta^\gamma\Big) - 1\Big\}\Big]\Big]^3}{6e} + \frac{e_o}{e}\Big[\Pi\Big[\lambda + \nu\Big\{\sqrt{3}tan\Big(\frac{\sqrt{3}}{2}\ mu\ \eta^\gamma\Big) - 1\Big\}\Big]\Big]. \tag{114}$$

For Family 18: When $\lambda = \mu = 0$,

$$y_{18}(x,t) = \frac{-2\sqrt{2}\Pi}{\eta^\gamma}, \tag{115}$$

$$z_{18}(x,t) = \frac{\Big[\frac{-2\sqrt{2}\Pi}{\eta^\gamma}\Big]^3}{6e} + \frac{e_o}{e}\Big[\frac{-2\sqrt{2}\Pi}{\eta^\gamma}\Big]. \tag{116}$$

For Family 19: When $\mu = \nu$ and $\lambda = 0$,

$$y_{19}(x,t) = \sqrt{\frac{2e_0\nu}{\mu}}\ tan\big(\mu\ \eta^\gamma\big), \tag{117}$$

$$z_{19}(x,t) = \frac{\Big[\sqrt{\frac{2e_0\nu}{\mu}}\ tan\big(\mu\ \eta^\gamma\big)\Big]^3}{6e} + \frac{e_o}{e}\Big[\sqrt{\frac{2e_0\nu}{\mu}}\ tan\big(\mu\ \eta^\gamma\big)\Big]. \tag{118}$$

4.2 Graphical depiction of solutions

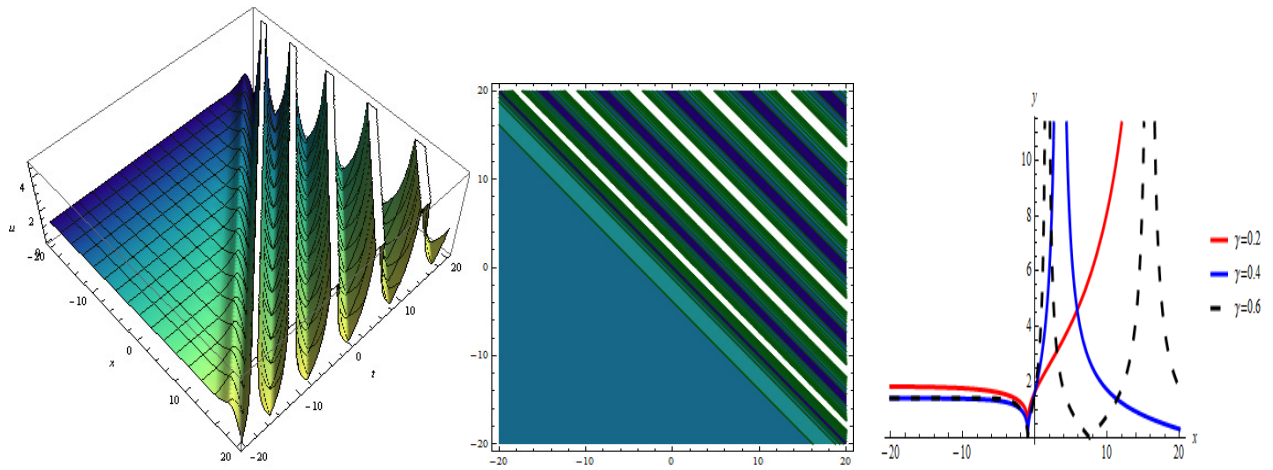

(a) (b) (c)

Figure 5: In these figure, we take $\lambda = \mu = \nu = 1$, $e_0 = 1$, $e = -1$, for the solution $y_{1,1}(x,t)$. (a) displays the 3D-plot of $y_{1,1}(x,t)$ with $\gamma = 0.8$. (b) displays the contour plot of the solution $y_{1,1}(x,t)$. (c) displays the 2D-plot of $y_{1,1}(x,t)$ for $t = 1$ with different values of γ.

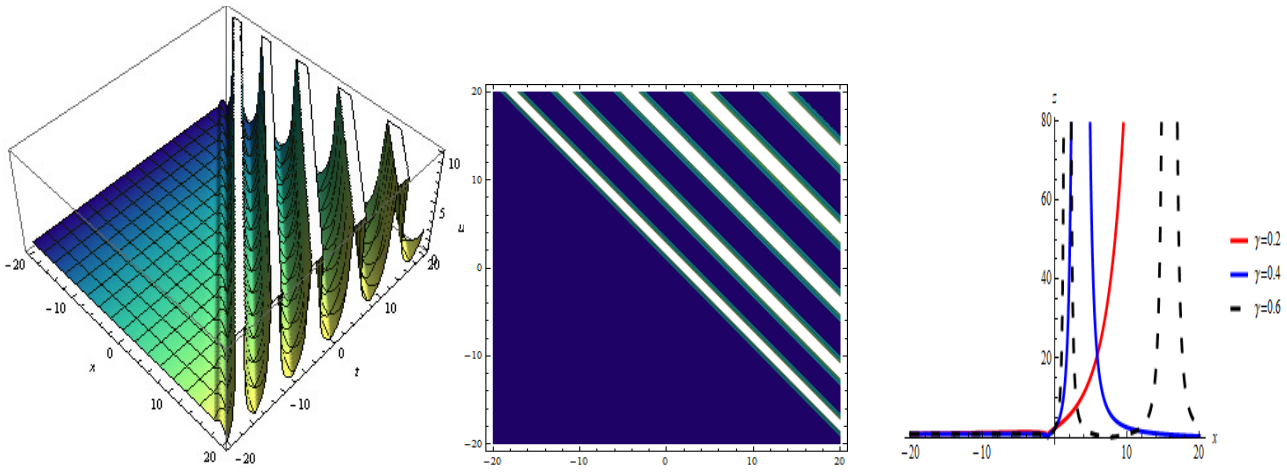

(a) (b) (c)

Figure 6: In these figure, we take $\lambda = \mu = \nu = 1$, $e_0 = 1$, $e = -1$, for the solution $z_{1,1}(x,t)$. (a) shows the 3D-plot of $z_{1,1}(x,t)$ with $\gamma = 0.8$. (b) displays the contour plot of the solution $z_{1,1}(x,t)$. (c) presents the 2D-plot of $z_{1,1}(x,t)$ for $t = 1$ with different values of γ.

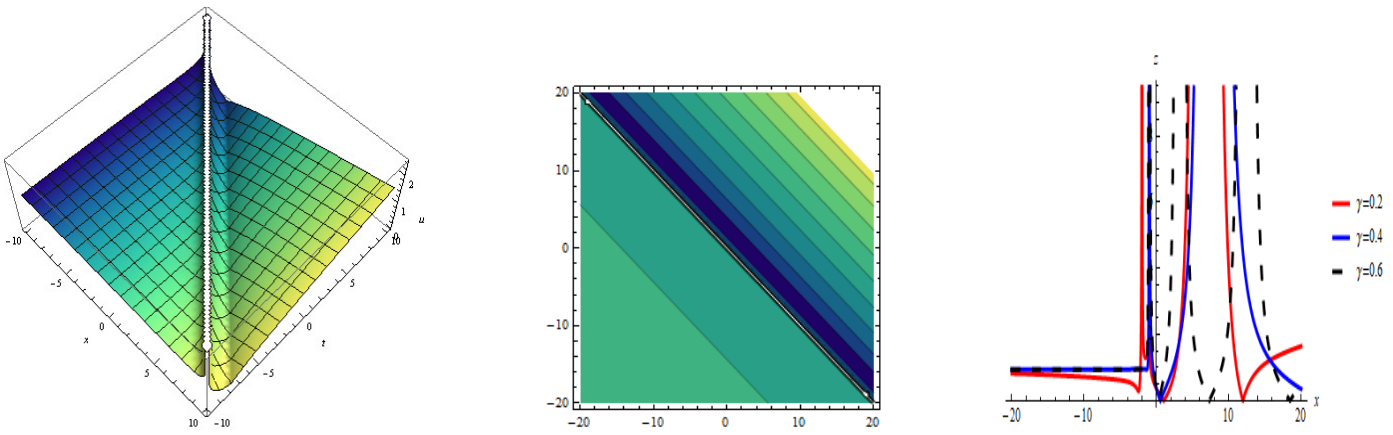

(a) (b) (c)

Figure 7: In these figure, we take $\mu = 2$, $\lambda = \nu = 1$, $e_0 = 1$, $e = -1$, for the solution $y_{1,2}(x,t)$. (a) shows the 3D-plot of $y_{1,2}(x,t)$ with $\gamma = 0.8$. (b) displays the contour plot of the solution $y_{1,2}(x,t)$. (c) displays the 2D-plot of $y_{1,2}(x,t)$ for $t = 1$ with different values of γ.

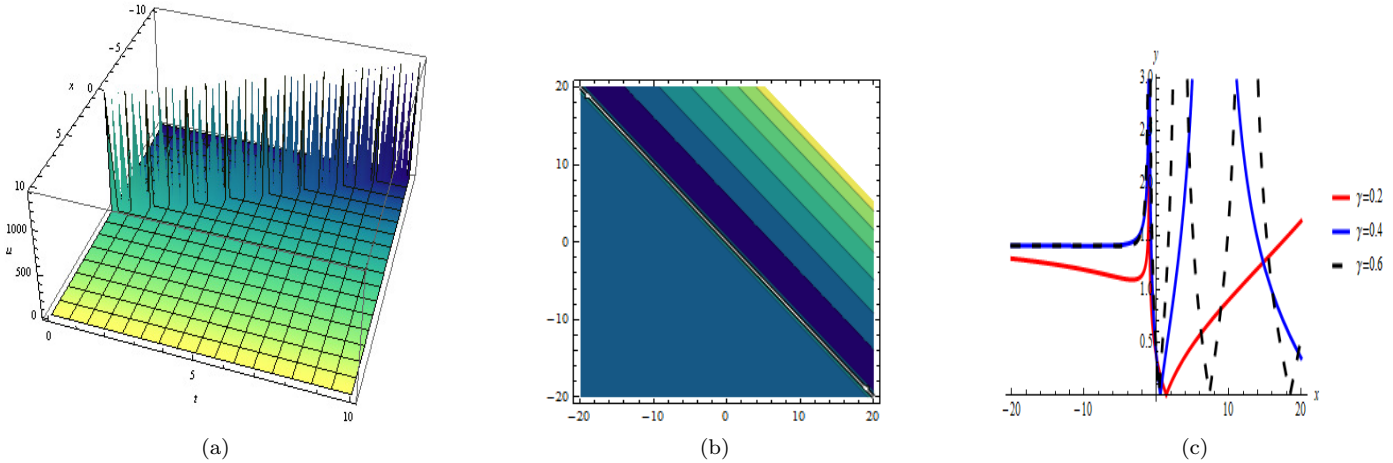

(a) (b) (c)

Figure 8: In these figure, we take $\mu = 2$, $\lambda = \nu = 1$, $e_0 = 1$, $e = -1$, for the solution $z_{1,2}(x,t)$. (a) shows the 3D-plot of $z_{1,2}(x,t)$ with $\gamma = 0.2$. (b) displays the contour plot of the solution $z_{1,2}(x,t)$. (c) presents the 2D-plot of $z_{1,2}(x,t)$ for $t = 1$ with different values of γ.

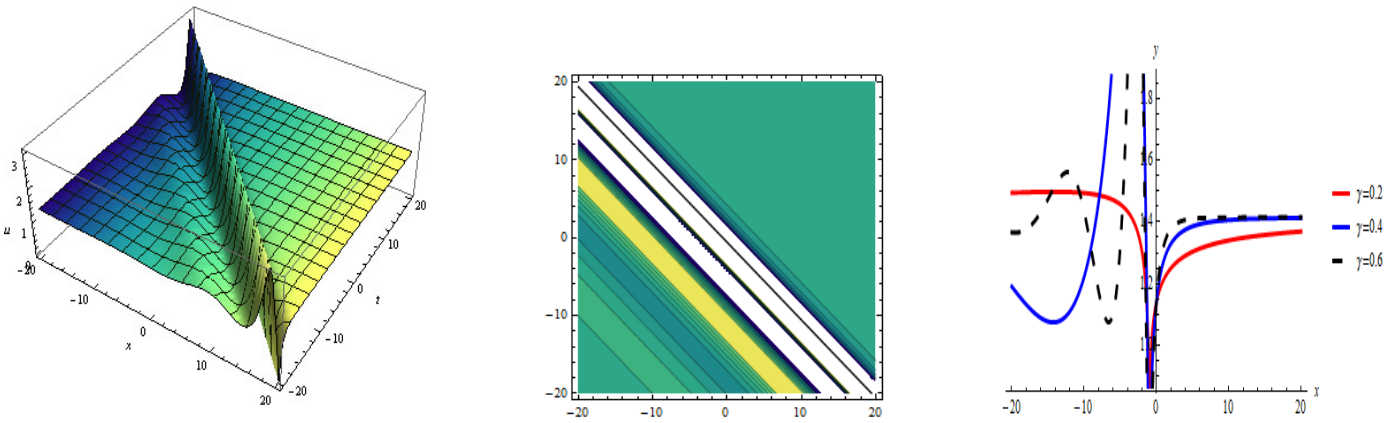

(a) (b) (c)

Figure 9: In these figure, we take $\lambda = 3$, $\mu = \nu = 1$, $e_0 = -1$, $e = -1$, for the solution $y_{2,1}(x,t)$. (a) shows the 3D-plot of $y_{2,1}(x,t)$ with $\gamma = 0.6$. (b) displays the contour plot of the solution $y_{2,1}(x,t)$. (c) presents the 2D-plot of $y_{2,1}(x,t)$ for $t = 1$ with different values of γ.

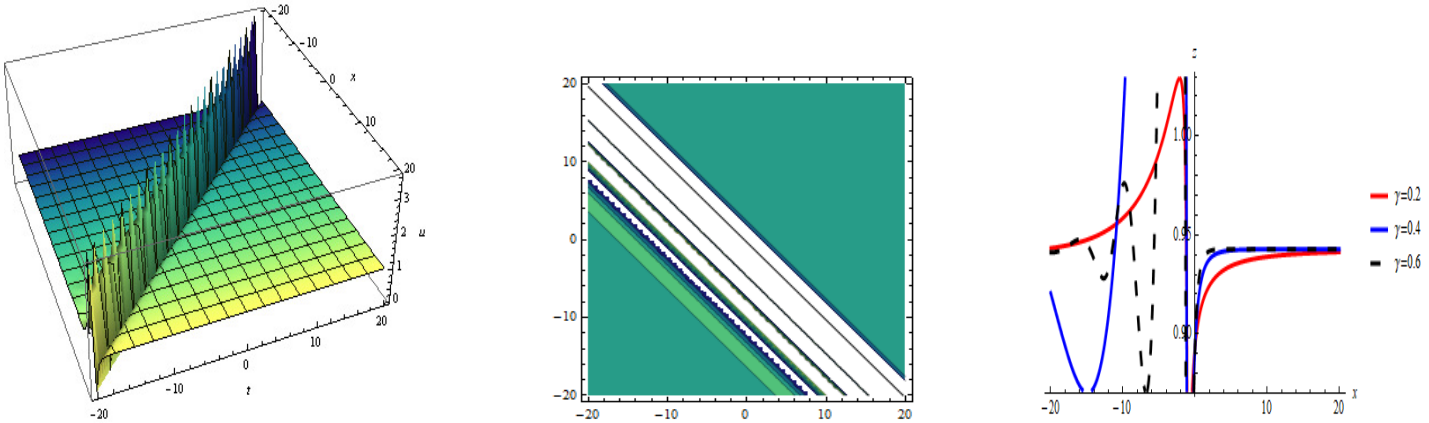

(a) (b) (c)

Figure 10: In these figure, we take $\lambda = 3$, $\mu = \nu = 1$, $e_0 = -1$, $e = -1$, for the solution $z_{2,1}(x,t)$. (a) shows the 3D-plot of $z_{2,1}(x,t)$ with $\gamma = 0.2$. (b) displays the contour plot of the solution $z_{2,1}(x,t)$. (c) presents the 2D-plot of $z_{2,1}(x,t)$ for $t = 1$ with different values of γ.

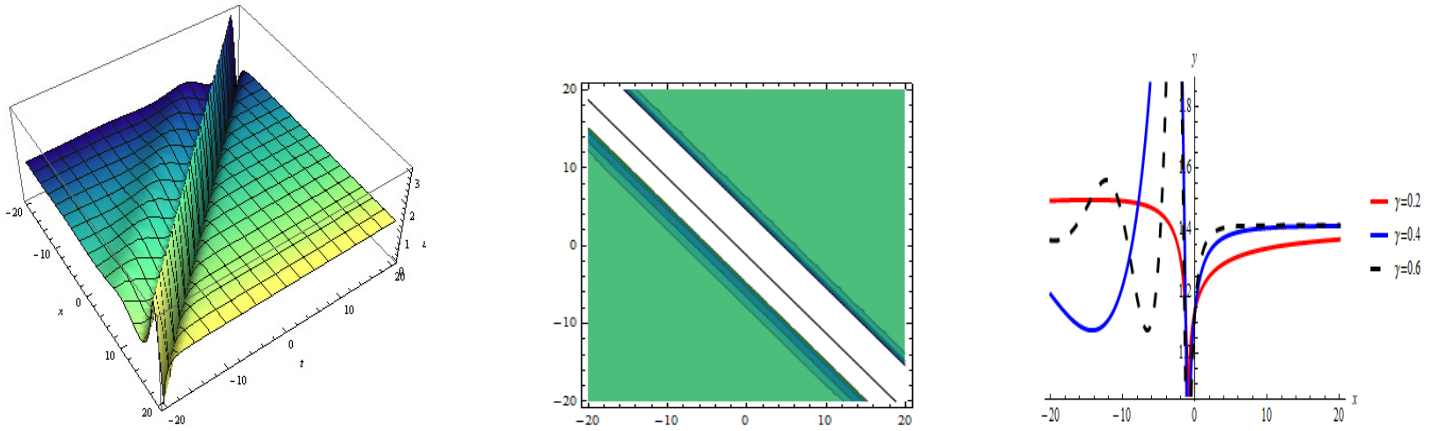

(a) (b) (c)

Figure 11: In these figure, we take $\lambda = \nu = 1$, $\mu = -1$ $e_0 = e = -1$, for the solution $y_{4,1}(x,t)$. (a) shows the 3D-plot of $y_{4,1}(x,t)$ with $\gamma = 0.4$. (b) displays the contour plot of the solution $y_{4,1}(x,t)$. (c) presents the 2D-plot of $y_{4,1}(x,t)$ for $t = 1$ with different values of γ.

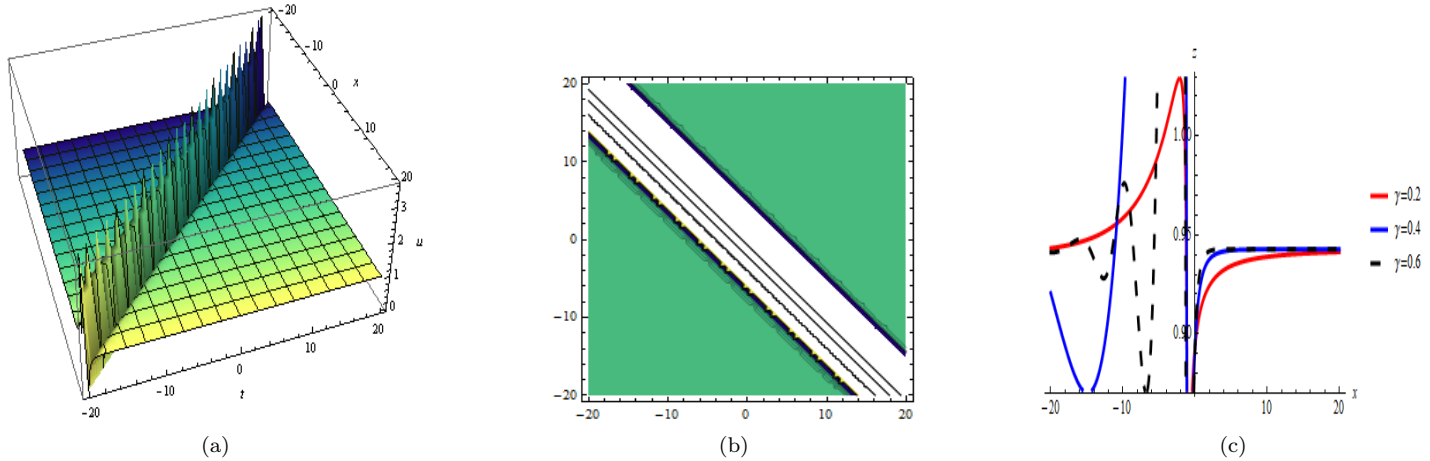

(a) (b) (c)

Figure 12: In these figure, we take $\lambda = \nu = 1$, $\mu = -1$ $e_0 = e = -1$, for the solution $z_{4,1}(x,t)$. (a) shows the 3D-plot of $z_{4,1}(x,t)$ with $\gamma = 0.8$. (b) displays the contour plot of the solution $z_{4,1}(x,t)$. (c) presents the 2D-plot of $z_{4,1}(x,t)$ for $t = 1$ with different values of γ.

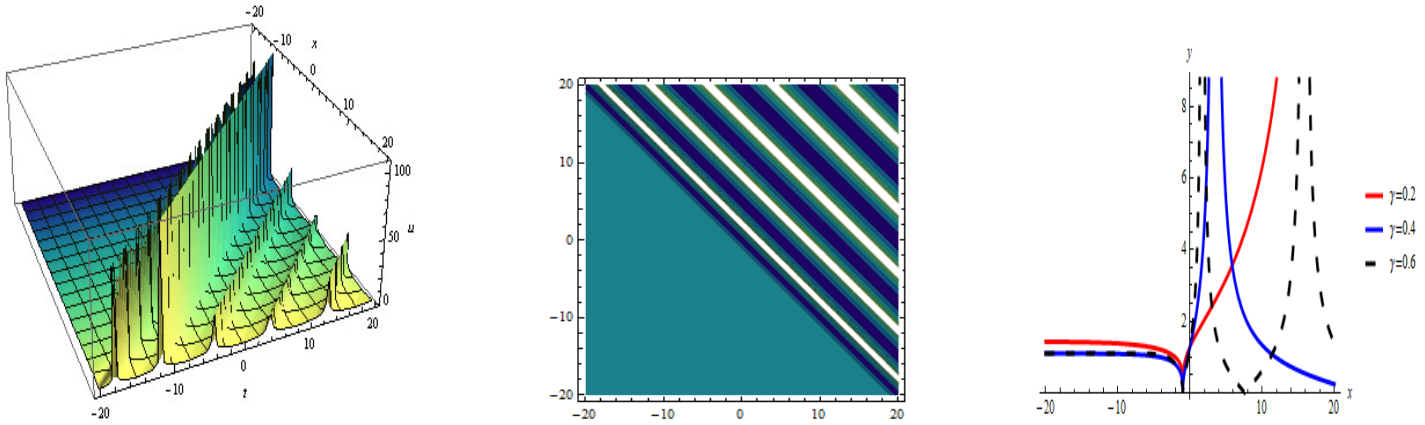

(a) (b) (c)

Figure 13: In these figure, we take $\lambda = \nu = 1$, $\mu = -1$ $e_0 = e = -1$, for the solution $y_{6,1}(x,t)$. (a) shows the 3D-plot of $y_{6,1}(x,t)$ with $\gamma = 0.8$. (b) displays the contour plot of the solution $y_{6,1}(x,t)$. (c) presents the 2D-plot of $y_{6,1}(x,t)$ for $t = 1$ with different values of γ.

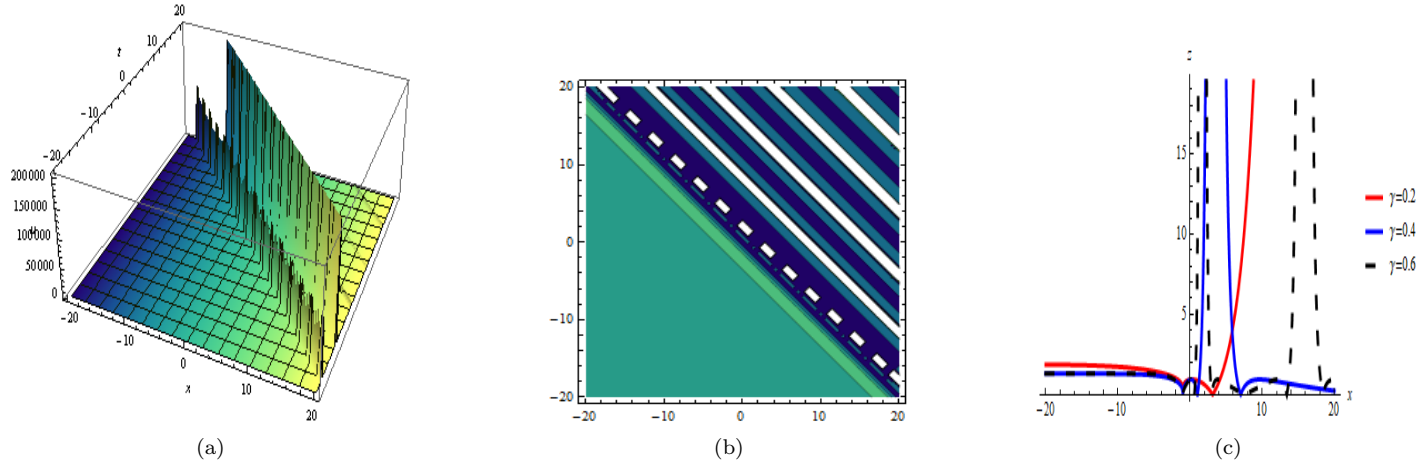

(a) (b) (c)

Figure 14: In these figure, we take $\lambda = \nu = 1$, $\mu = -1$ $e_0 = e = -1$, for the solution $z_{6,1}(x,t)$. (a) shows the 3D-plot of $z_{6,1}(x,t)$ with $\gamma = 0.8$. (b) displays the contour plot of the solution $z_{6,1}(x,t)$. (c) presents the 2D-plot of $z_{6,1}(x,t)$ for $t = 1$ with different values of γ.

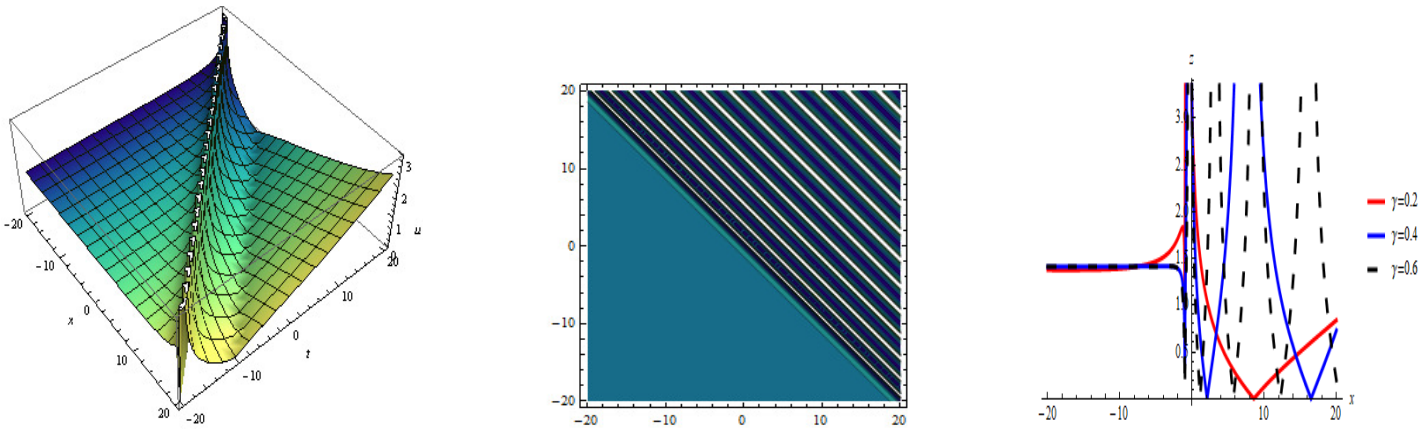

(a) (b) (c)

Figure 15: In these figure, we take $\lambda = 1$, $\nu = 2$, $\mu = -2$ $e_0 = e = -1$, for the solution $y_{19}(x,t)$. (a) shows the 3D-plot of $y_{19}(x,t)$ with $\gamma = 0.8$. (b) displays the contour plot of the solution $y_{19}(x,t)$. (c) presents the 2D-plot of $y_{19}(x,t)$ for $t = 1$ with different values of γ.

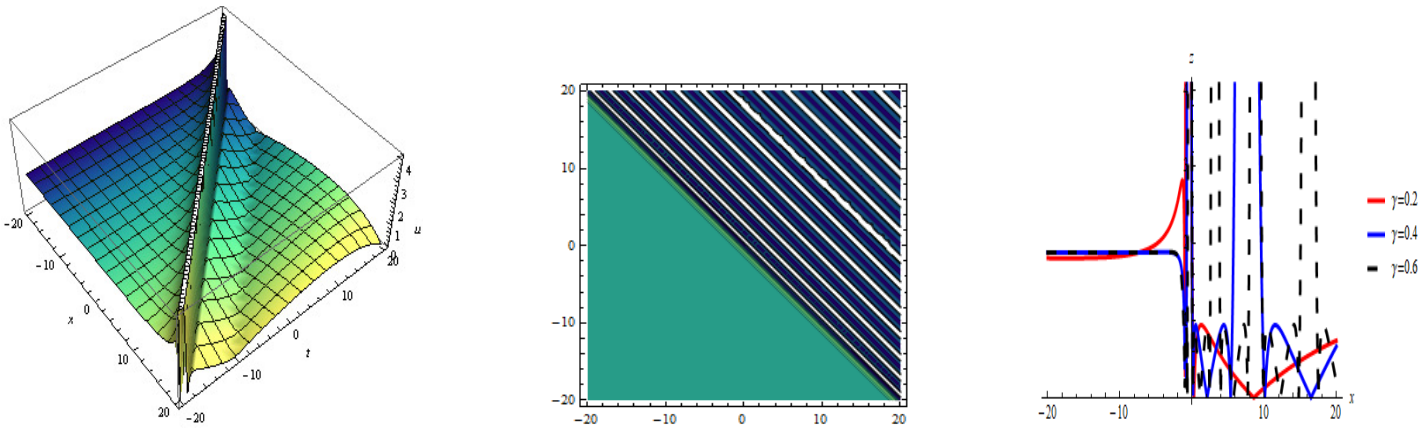

(a) (b) (c)

Figure 16: In these figure, we take $\lambda = 1$, $\nu = 2$, $\mu = -2$ $e_0 = e = -1$, for the solution $z_{19}(x,t)$. (a) shows the 3D-plot of $z_{19}(x,t)$ with $\gamma = 0.8$. (b) displays the contour plot of the solution $z_{19}(x,t)$. (c) presents the 2D-plot of $z_{19}(x,t)$ for $t = 1$ with different values of γ.

5 Results and Discussion

In this paper, we have practiced two effective integration approaches to the KMM model, one is the Semi-inverse method and the other is NAEM. The first method provides us bright solitons in the form of Eq.(23), Eq.(24), Eq.(33) and Eq.(34). Also the graphical interpretation for the absolute behavior of these solutions by assigning different parameter values is given in section 3.1. Bright solitons in the form of 3D, contour and 2D plots are given in Figs.1,2,3 and 4. 2D graphs are displaying fractal effect for the parameter values $\gamma = 0.2, 0.4, 0.6, 0.8$ on the solutions.

The preceding method presents dual-mode bright, dark, singular-periodic and singular-shaped solitons in Eq.[73-118] for the governing system. This section consists of 3D, contour and 2D graphs of the mentioned solutions

with their physical significance. The fractal impact is illustrated by the irregularity in the curves for various values of parameter $\gamma = 0.2, 0.4, 0.6$ on the solutions. From the graphs, it is clear that the semi-inverse technique and NAEM may be applicable to any coupled nonlinear partial differential equation for the extraction of bright and dual-mode solitary waves solutions, correspondingly. It is worth mentioning here that the above approaches are efficient, versatile and powerful to acquire the solitons with real-world applications.

6 Conclusion

The study of optical solitons is discussed in this article by applying semi inverse and NAEM. The exact dark, bright, singular-periodic and singular-shaped soliton solutions of the KMM model are developed, having significance in mathematics and physics. The fractal KMM system is of great importance and used for describing ferromagnetic particle propagation in nano-scale ferrite materials. A new collection of solutions is investigated with several of them being envisioned. The set of soliton from this analysis is effective to understand properties of the governing system of equations. The results obtained are compared with the existing literature and found to be new [27]. These consequences may be important for the future work of the given model. It should be noted that, in contrast to other algebraic approaches, semi-inverse method and the NAEM revealed a variety of additional advantages for optical solitons. These results have been represented graphically in figures to understand the physical importance.

References

[1] Zabel, H., Superlattice Microstruct, 46, 541 (2009).

[2] Shen, B.G., Sun, J.R., Hu, F.X., Zhang, H.W., Cheng, Z.H., Recent Progress in Exploring Magnetocaloric Materials, Advanced Materials, 21, 4545 (2009).

[3] Tanaka, M., Ohya, S., Hai, P.N., Recent progress in III-V based ferromagnetic semiconductors: Band structure, Fermi level, and tunneling transport, Applied Physics Reviews, 1, 011102 (2014).

[4] Newman, N., Wu, S.Y., Liu, H.X., Recent progress towards the development of ferromagnetic nitride semiconductors for spintronic applications, Physica Status Solidi A, 203, 2729 (2006).

[5] Tang, J.S., Wang, K.L., Electrical spin injection and transport in semiconductor nanowires: challenges, progress and perspectives, Nanoscale, 7, 4325 (2015).

[6] Bazaliy, Y.B., Jones, B.A., Zhang, S.C., Modification of the Landau-Lifshitz equation in the presence of a spin-polarized current in colossal- and giant-magnetoresistive materials, Physical Review B, 29, 2137 (2012).

[7] Fairouz Tchier, Mustafa Inc, Bulent Kilic, Ali Akgül, On soliton structures of generalized resonance equation with time dependent coefficients, Optik, Volume 128, 2017, Pages 218-223, ISSN 0030-4026,

[8] Hashemi, M.S., Inc, M., Kilic, B., Akgül, A., On solitons and invariant solutions of the Magneto-electro-elastic circular rod, Waves in Random and Complex Media, 26, (2016), 259-271.

[9] Raza, N Javid, A., Generalization of optical solitons with dual dispersion in the presence of Kerr and quadratic-cubic law nonlinearities, Modern Physics Letters B, 33, 1850427 (2019).

[10] Raza, N., Javid, A., Optical dark and dark-singular soliton solutions of (1+2)-dimensional Chiral Nonlinear Schrodinger Equation, Waves in Random and Complex Media, 29, 496-508 (2018).

[11] Raza, N., Abdullah, M., Butt, A.R., Murtaza, I.G., Sial, S., New exact periodic elliptic wave solutions for extended quantum Zakharov-Kuznetsov equation, Optical Quantum Electronics (2018) 50:177 doi.org/10.1007/s11082-018-1444-x.

[12] ue Guan, Wenjun Liu, Qin Zhou, Anjan Biswas, Some lump solutions for a generalized (3+1)-dimensional Kadomtsev?Petviashvili equation, Applied Mathematics and Computation, Volume 366, 2020, 124757,

[13] Younis, M., Bilal, M., Rehman, S.U., Younas, U., Rizvi, S.T.R.,Investigation of optical solitons in birefringent polarization preserving fibers with four-wave mixing effect, International Journal of Modern Physics B, 34, 2050113 (2020)

[14]] Osman, M.S., Multi-soliton rational solutions for some nonlinear evolution equations, Open Physics, 14, 26 (2016).

[15] Abdul-Majid Wazwaz, Study on a New (3+1)-Dimensional Extensions of the Konopelchenko-Dubrovsky Equation, Appl. Math. Inf. Sci. 12, (2018) 1067-1071.

[16] Iqbal, M., Seadawy, A.R., Khalil, O.H., Lu, D., Propagation of long internal waves in density stratified ocean for the (2+ 1)-dimensional nonlinear Nizhnik-Novikov-Vesselov dynamical equation Results in Physics, 16, 102838 (2020).

[17] Raza, N., Zubair, A., Dipole and combo optical solitons in birefringent fibers in the presence of four wave mixing, Commun. Theor. Phys. 71, (2019) 723-730.

[18] Chen Yue, Dianchen Lu, Mostafa MA Khater, Abdel-Haleem Abdel-Aty, W Alharbi, Raghda AM Attia, On explicit wave solutions of the fractional nonlinear DSW system via the modified Khater method, Fractals, Vol. 28, No. 08, 2040034 (2020).

[19] Khater, M.M.A., Attia, R.A.M., and Abdel-Aty, A., Computational analysis of a nonlinear fractional emerging telecommunication model with higher?order dispersive cubic?quintic, Information Sciences Letters 9, (2020) 83-93.

[20] D. Kumar, C. Park, N. Tamanna, G.C. Paul and M.S. Osman, Dynamics of two-mode Sawada-Kotera equation: Mathematical and graphical analysis of its dual-wave solutions, Results in physics 19, (2020) 103581.

[21] Atangana, A., Modelling the spread of COVID-19 with new fractal-fractional operators: Can the lockdown save mankind before vaccination, Choas, Solitons and Fractals, 136, (2020), 109860.

[22] Owolabi, K.M., Atangana, A., Akgul, A., Modelling and analysis of fractal-fractional partial differential equations: Application to reaction-diffusion model, Alexandria Engineering Journal, 59, (2020), 2477-2490.

[23] Atangana, A., Fractal-fractional differentiation and integration: Connecting fractal calculus and fractional calculus to predict complex system, Choas, Solitons and Fractals, 102, (2017), 396-406.

[24] He, J.H., Variational Principles for some Nonlinear Partial Differential Equation with Variable coefficients, Chaos, Solitons and Fractals, 19, 847-851 (2004)

[25] Liu, S., Zhou, Q., Biswas, A., Liu, W., Phase-Shift controlling of three solitons in dispersion-decreasing fibers, Non-linear Dynamics, 98, 395-340, (2019).

[26] Fan, X., Qu, T., Huang, S., Chen., X., Cao,M., Zhou, Q., Liu, W., Analytic study on the influences of the higher-order effects on optical solitons in fiber laser, Optik, 186, 326-331 (2019).

[27]]Kraenkel,R.A., Manna, M.A., Merle,V., Nonlinear short-wave propagation in ferrites, Physical Review E, 61, 976 (2000).

[28] Nguepjouo, F.T., Kuetche, V.K., Kofane, T.C., Soliton interactions between multivalued localized waveguide channels within ferrites, Physical Review E, 89, 063201 (2014).

[29] Khan, Y., Faraz, N., Yildrim, A., New soliton solutions of generalized Zakharov equations using He's Variational approach, Applied Mathematics Letters, 24, 965-968 (2011).

[30] Khan, Y., A new necessary condition of soliton solutions for Kawahara equation arising in physics, Optik, 155, 273-275 (2018).

[31] He, J.H., Variational principles for some nonlinear partial differential equations with variable coefficients, Chaos, Solitons and Fractals, 19, 847-851 (2004).